



# 4.

## COMPACTING OF METAL POWDERS

*In order to fully comprehend the possibilities and limitations of powder compacting, it is necessary not only to study the empirical phenomena of this process, but also to reveal the basic mechanisms behind them.*

## **TABLE OF CONTENTS**

Introduction

4.1 Density - Porosity - Compacting Pressure

4.2 Radial Pressure - Axial Pressure

4.3 Axial Density Distribution

4.4 Ejecting Force and Spring-Back

References

## Introduction

The forming of a sintered component begins with the densification of the metal powder in a rigid die having a cavity of more or less complicated contour. In this operation, high pressures (usually  $650 \text{ N/mm}^2$ ) are exerted upon the powder in the die cavity, simultaneously from top and bottom, via two or more vertically moving compacting punches.

Under the influence of such high compacting pressures, the powder particles are being squeezed together so closely that their surface irregularities interlock and a certain amount of cold welding takes place between their surfaces.

After ejection from the die, if the compacting operation was successful, the compact owns sufficient strength (so-called green-strength) to withstand further handling without damage. In order to facilitate the compacting operation and reduce tool-wear to a minimum, a lubricant is admixed to the powder before compacting.

In order to fully comprehend the possibilities and limitations of powder compacting, it is required not only to study the empirical phenomena of this process, but also to reveal the basic mechanisms behind them.

## 4.1 Density - Porosity - Compacting Pressure

At first, some definitions are required:

- **Specific Weight:**  $\rho = m/V_t$  (measured in  $\text{g/cm}^3$ );  $m$  = mass of the material;  $V_t$  = true volume of the material.
- **Density:**  $\delta = m/V_b$  (measured in  $\text{g/cm}^3$ );  $m$  = mass of the powder resp. compact;  $V_b$  = bulk volume (enveloping volume).
- **Theoretical Density:**  $\delta_{th}$  = density of a (practically not attainable) pore-free powder compact (measured in  $\text{g/cm}^3$ ).
- **Porosity:**  $\phi = 1 - \delta/\delta_{th}$  (number without dimension).
- **Compacting Pressure (die compacting):**  $P$  = compacting force/face area of compact (measured in  $\text{N/mm}^2$  or  $\text{MN/m}^2$ ).
- **Compacting Pressure (isostatic compacting):**  $P$  = pressure of the hydraulic medium (measured in  $\text{MPa}$  or  $\text{MN/m}^2$ ).

#### 4.1.1 Empirical Density-Pressure Curves

##### Powder Compacting in a Cylindrical Die.

The strength properties of sintered components increase with increasing density but their economy drops with increasing energy input and increasing load on the compacting tool. Thus, it is most desirable, for both economic and technical reasons, to achieve the highest possible compact density at the lowest possible pressure.

Density-pressure curves give information about the frame within which a suitable compromise may be found. These curves are generally obtained from standard laboratory tests where a number of compacts are made at different pressures in a carbide die having a cylindrical bore of 25 mm diameter. The densities of the compacts are plotted against compacting pressures. The diagram at *Fig. 4.1* shows density-pressure curves for two commercial iron powders (NC100.24 and ASC100.29).

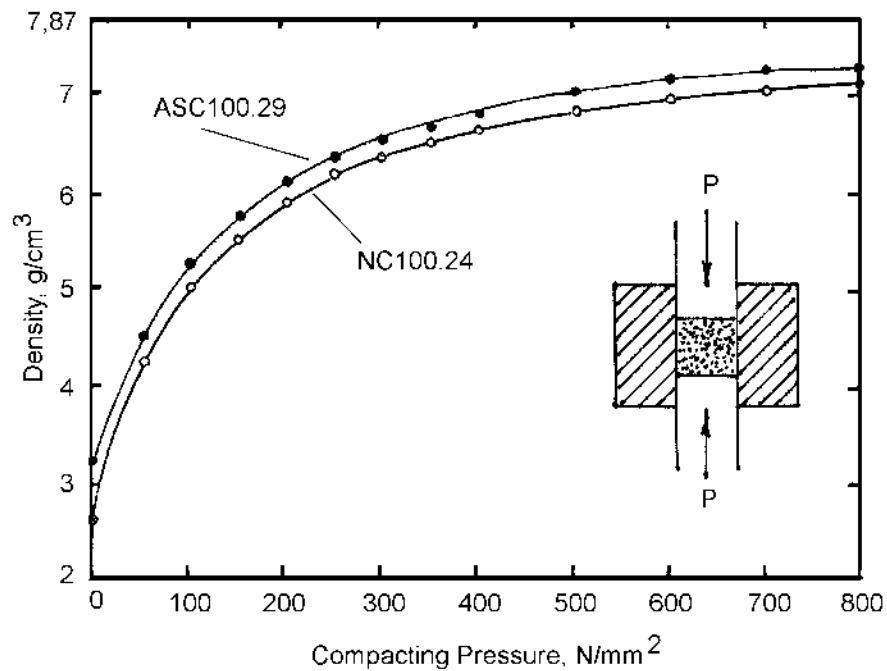


Fig. 4-1. Density-pressure curves for two commercial iron powders compacted in a carbide die having an inner diameter of 25 mm. Lubricant additions: 0.75% Zn-stearate. [4.1]

A striking feature of these curves is the fact that their slope decreases considerably with increasing compacting pressures, and that the density of massive pure iron ( $7.86 \text{ g/cm}^3$ ) obviously cannot be reached at feasible pressures. We notice, further, that the two iron powders despite their chemical identity yield different density-pressure curves. This different compacting behavior arises from differences of their particle structure. See Chapter 3.

### Isostatic Powder Compacting.

A powder under isostatic pressure shows a similar densification behavior as in die-compacting. This is illustrated by the following example: Samples of electrolytic iron powder, hermetically enclosed in thin rubber jackets and embedded in a hydraulic medium, were subjected to varying isostatic pressures.

Since there is no die-wall friction in isostatic compacting, the powder was not admixed with any lubricants. The so obtained densification curves are shown at *Fig. 4.2*, and the microstructures of some of the compacts are shown at *Fig. 4.3*.

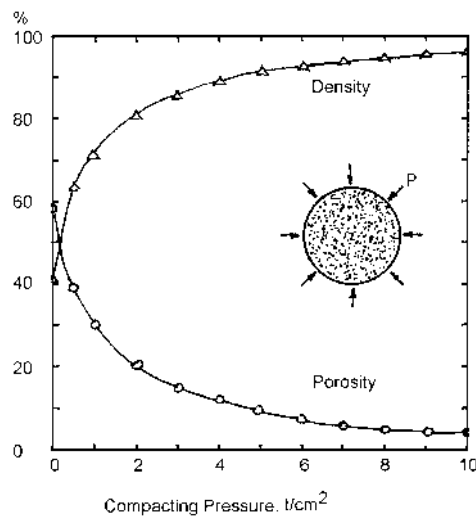


Figure. 4.2. Relative density and porosity as functions of isostatic compacting pressure. Electrolytic iron powder hermetically enclosed in thin rubber jackets subjected to hydraulic pressure. [4.2]

The following details are noticed from these microstructures:

- At a density of  $5.56 \text{ g/cm}^3$  (29.2% porosity), many pores are still of approx. the same size as the largest powder particles.
- At densities above  $6.17 \text{ g/cm}^3$  (21.5% porosity), powder particles are blocking each other to such degree that particle rearrangement is now entirely unlikely without severe plastic deformation of the particle (as may have occurred at lower densities).

#### 4. COMPACTING OF METAL POWDERS

---

- At densities above  $6.61 \text{ g/cm}^3$  (15.9% porosity), the largest remaining pores are much smaller than the largest powder particles, and at a density of  $7.44 \text{ g/cm}^3$  (5.3% porosity), all remaining pores are smaller than the smallest of the initial powder particles.

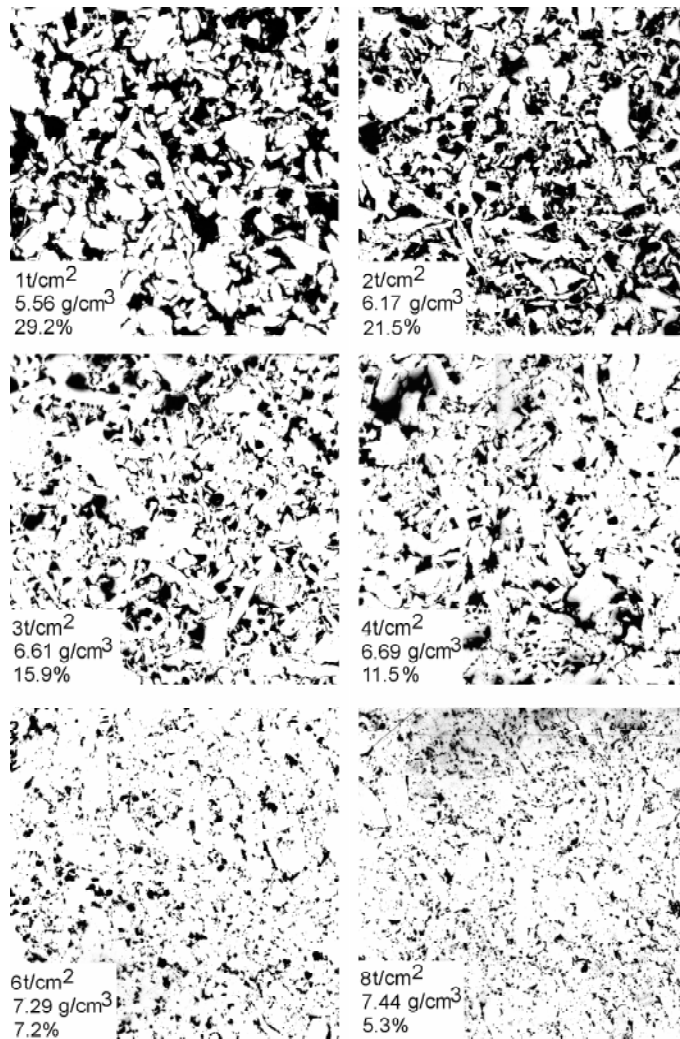


Figure. 4.3. Microstructures of some of the isostatically compacted samples used to establish the curves shown at Fig. 4.2. [4.3]

Adaptation of contact areas between adjacent powder particles, caused by plastic deformation, can be seen from the microstructure of a copper powder compact shown at *Fig. 4.4*. From this microstructure, it can also be seen that bigger powder particles form bridges around much smaller particles which thus, have escaped deformation.

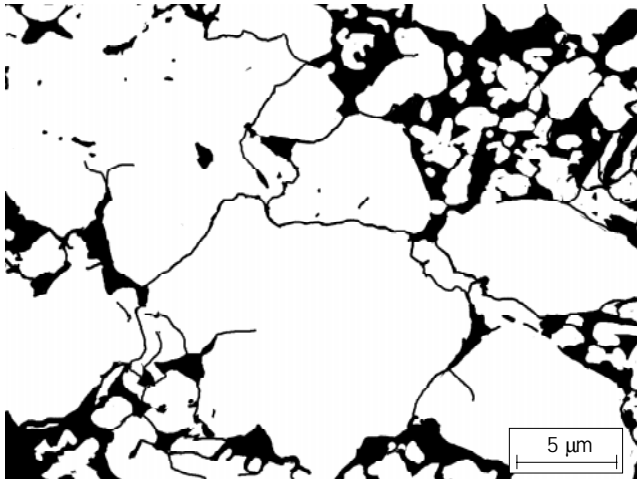


Figure. 4.4. Adaptation of surface contours due to plastic deformation of adjacent powder particles. Electrolytic copper powder compacted at 200 N/mm<sup>2</sup>. [4.4]

#### 4.1.2 Principle Limits to Densification

Since early in the 1930's, powder metallurgists have endeavored to find a suitable mathematical description of the process of powder densification. The number of formulae which to this effect have been suggested over the last three decades is legion. However, non of these formulae, most of them extracted from simple curve-fitting exercises, has proven to be sufficiently universal and substantiated by general physical principles to be acceptable as sound theory of powder densification.

In work shop practice, such formulae are dispensable because it is far more reliable and hardly more tedious to establish relevant densification curves experimentally than to calculate them from complicated and questionable formulae.

On the other hand, it is quite useful to understand, in principle at least, in which way the process of powder densification is influenced and limited by general laws of physics and mechanics.

##### **Deformation Strengthening of Powder Particles.**

Disregarding, for the moment, the problem of wall friction in die-compacting and considering isostatic compacting of powder only, we recognize that the problem of powder densification arises from an underlying physical problem which can be defined as follows:

- With increasing densification, the powder particles are plastically deformed and increasingly deformation strengthened, i.e. their yield point is steadily being raised.
- Simultaneously, the contact areas between particles are increasing and, consequently, the effective shearing-stresses inside the particles are decreasing. Thus, at constant external pressure, decreasing shearing-stresses meet a rising yield point, and all further particle deformation ceases, i.e. the densification process stops.

The deformation strengthening of the powder particles can be made evident by means of X-ray structural analysis. At *Fig. 4.5*, three photo-records of X-ray back-reflections are shown, obtained (A) from a commercial sponge-iron powder, (B) from a compact of this powder pressed at  $290 \text{ N/mm}^2$ , and (C) from the same compact after soft-annealing for 2 minutes at  $930^\circ\text{C}$ .

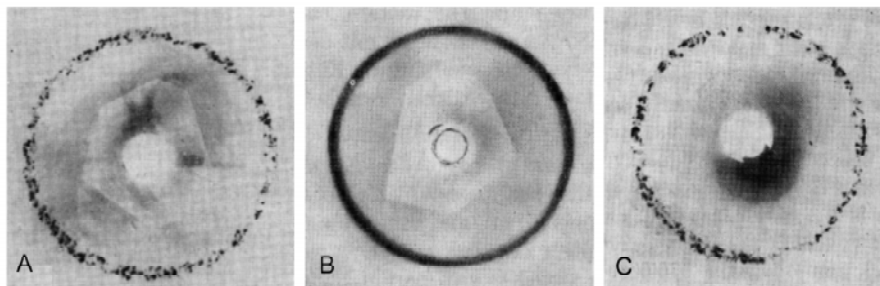


Figure. 4.5. Deformation strengthening of powder particles in the compacting of sponge iron powder (Höganäs NC100.24). Photographic records of X-ray back-reflections (Cr-K $\alpha$  radiation, V-filter). (A) powder before compacting, (B) compact made at  $3 \text{ t/cm}^2$ , (C) the same compact after soft-annealing for 2 minutes at  $930^\circ\text{C}$ . [4.5]

The distinct X-ray reflections (sharp black spots) on photo-records (A) and (C) give evidence of undisturbed crystal lattices in powder particles free from deformation-strengthening. The diffuse ring-shaped X-ray reflection on photo-record (B) gives evidence of severely disturbed crystal lattices in deformation-strengthened powder particles.



**Decrease of Maximum Shearing Stress.**

In a state of densification where the powder particles are squeezed together to such extent that the initially interconnected pores between them have degenerated to small isolated pores, the stress distribution around each of them can be fairly well approximated by the stress distribution in a hollow sphere under hydrostatic outside pressure  $P$ . Let the hollow sphere be of metal having a yield-point  $\sigma_0$ . Let  $R$  be the outer radius of the sphere and  $r$  its inner radius.

According to theory of elasticity, plastic deformation will occur when the maximum shearing stress  $\tau_m$  at the outer surface of the hollow sphere exceeds the shearing yield-stress  $\tau_0 = \sigma_0/2$ , i.e. when  $\tau_m(R) \geq \sigma_0/2$ . See sketch at *Fig. 4.6*. From the principle of *Mohr's circle* we derive the general relationship  $\tau_m = (\sigma_r - \sigma_t)/2$ . Thus the condition of plastic flow for the hollow sphere is:

$$\sigma_r(R) - \sigma_t(R) \geq \sigma_0 \quad (4.1)$$

The radial stress  $\sigma_r(R)$  and the tangential stress  $\sigma_t(R)$  close to the outer surface of the hollow sphere are given by the following relations:

$$\sigma_r(R) = -P \quad (4.2)$$

and

$$\sigma_t(R) = -P \frac{2R^3 + r^3}{2(R^3 - r^3)} \quad (4.3)$$

Introducing (4.2) and (4.3) into (4.1) yields:

$$P \frac{3r^3}{2(R^3 - r^3)} \geq \sigma_0 \quad (4.4)$$

or:

$$P \geq \frac{2}{3} \sigma_0 \frac{R^3 - r^3}{r^3} \quad (4.5)$$

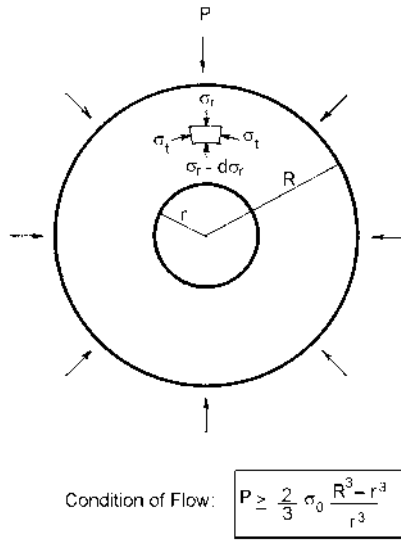


Figure. 4.6. Condition of plastic flow in a hollow sphere of metal under hydraulic outside pressure P.

R = outer diameter, r = inner diameter,  
 $\sigma_0$  = yield point of the metal,  $\sigma_r$  = radial stress,  
 $\sigma_t$  = tangential stress.

According to equation (4.5), the hydrostatic pressure P, required to provoke plastic deformation of the hollow sphere, is the higher the smaller the volume of the hole ( $\sim r^3$ ) is relative to the metal volume of the sphere ( $\sim R^3 - r^3$ ). In other words: an infinitely high pressure would be required to reduce the hole inside the metal sphere to nothing.

Transferring this result analogously to the small isolated pores inside a highly densified powder compact, it appears plausible that these small pores cannot be eliminated by means of feasible pressures - not even in the absence of deformation strengthening. At constant external pressure, the maximum shearing stress anywhere in the compact is the smaller, the smaller the residual pores are.

#### Theoretical Density of Powder Mixes.

Sintered components are usually manufactured from mixes of unalloyed or low-alloyed iron powder with additives like graphite, other metal powders and lubricants. Compact densities attainable with such powder mixes are, of course, influenced by the specific weights and the relative amounts of the additives and of impurities if any. The (only theoretically achievable) pore-free density  $\delta_M$  of a powder mix can be calculated as follows:

$\rho_{Fe}$  be the specific weight of the iron powder (base powder),

$w_{Fe}$  be the weight percentage of the iron powder,

$\rho_1, \rho_2, \rho_3, \dots$  be the specific weights of additives and impurities,

$w_1, w_2, w_3, \dots$  be the weight percentages of additives and impurities.

Then, the theoretically achievable pore-free density of the powder mix is:

$$\delta_M = 100 / (w_{Fe}/\rho_{Fe} + w_1/\rho_1 + w_2/\rho_2 + w_3/\rho_3 + \dots) \quad (4.6)$$

In Table 4.1, the specific weights are given of some additives and impurities as occurring in iron powder mixes. Using the data from this table and equation (4.6), the theoretical densities of various powder mixes on the basis of ASC100.29 have been calculated and plotted as functions of the relative amounts of the respective additives in the diagram shown at *Fig. 4.7*.

From the diagram emerges that added lubricants (indispensable for the reduction of die-wall friction) have the most lowering effect on the theoretical density of powder mixes. In the compacting process, part of the added lubricant is being squeezed towards the die-wall where it fulfills its intended function.

The remaining part of the lubricant gets entrapped inside closed pores where it develops a hydraulic pressure opposing the densification process.

**Table 4.1. Specific Weights of some Metals,  
Additives and Impurities as occurring in Iron Powder Mixes**

Metal, Additive, Impurity	Specific Weight (g/cm <sup>3</sup> )	Metal, Additive	Specific Weight (g/cm <sup>3</sup> )
Fe (purest iron)	7,868	NC 100.24	7,796
FeO	5,30	SC 100.26	7,807
SiO <sub>2</sub>	2,30	ASC 100.29	7,845
Graphit	2,24	MnS	4,0
Cu (electrolytic)	8,95	Ni (pure nickel)	8,902
Zn-stearate	1,0	synthetic wax	1,0

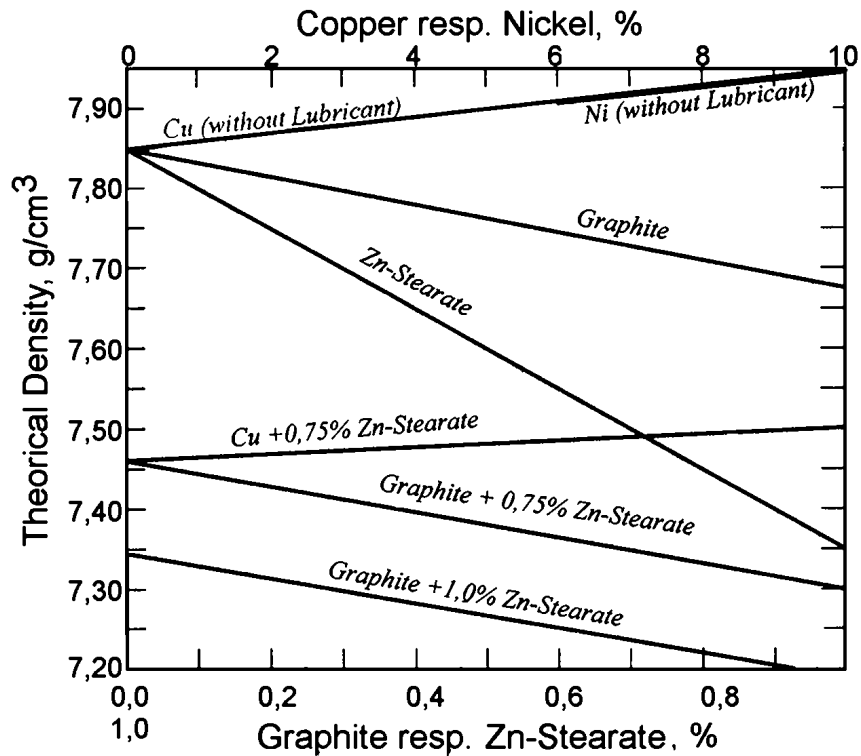


Figure. 4.7. Influence of added alloying elements and lubricants on the theoretical (pore-free) density of iron powder mixes based on ASC100.29.

Density-pressure curves, established in the laboratory according to standard compacting procedures, are useful guide lines for the approximate dimensioning of compacting tools. But they do not allow accurate predictions of pressures and densities to be expected when compacting complicated structural parts in dies with deep and narrow filling spaces (viz. gears and long thin-walled bushings).

In such instances, only carefully conducted compacting tests in the actual die can give reliable information.

## 4.2 Radial Pressure - Axial Pressure

When the piston of a hydraulic cylinder exerts pressure upon the liquid inside the cylinder, the pressure applied in axial direction is transformed 1:1 to radial pressure upon the cylinder wall. When a powder is being compacted in a rigid cylindrical die, the axial pressure, exerted upon the powder by the compacting punch, is only partly transformed to radial pressure upon the die wall.

This radial pressure can be quite substantial, but it cannot reach the level of the axial pressure because a powder is no liquid and has no hydraulic properties.

### 4.2.1 Hysteresis of the Radial Pressure

The way in which the empirical relationship between radial and axial pressure is governed by general laws of physics and mechanics can be understood, in principle at least, from a simple model, suggested in 1960 by W.M. Long<sup>1</sup>, and presented in detail below. First, we consider a free-standing cylindrical plug of metal having a modulus of elasticity  $E$  and a Poisson factor  $\nu$ . A compressive axial stress  $\sigma_a$ , applied to the end-faces of the plug, provokes, by laws of elasticity, a radial stress  $\sigma_r$ , and the radius of the plug is expanded by the factor

$$\varepsilon_r = (\sigma_r - \nu\sigma_r - \nu\sigma_a)/E \quad (4.7)$$

We now imagine the same plug being put into a tightly fitting cylindrical die. The die is assumed to have a modulus of elasticity much larger than that of the metal plug. Further, it is assumed that the die is extremely well lubricated, such that any friction between the plug and the die-wall is negligible. Exerting, via two counteracting punches, axial pressure upon the plug, its radial expansion  $\varepsilon_r$  is negligibly small because the die expands extremely little due to its large modulus of elasticity. Thus,  $\varepsilon_r = 0$  is a sufficiently close approximation of reality, and from (4.7), it follows:

$$\sigma_r - \nu\sigma_r - \nu\sigma_a = 0 \quad (4.8)$$

Hence, the relationship between radial and axial stress in the plug is:

$$\sigma_r = \sigma_a \nu / (1 - \nu), \text{ elastic loading} \quad (4.9)$$

---

<sup>1</sup>W.M. Long, Powder Metallurgy, No. 6, 1960.

The maximum shearing-stress in the plug (derived from Mohr's circle) is always :

$$\tau_{\max} = (\sigma_a - \sigma_r)/2 \quad (4.10)$$

With increasing axial stress in the plug,  $\tau_{\max}$  increases too, until it exceeds the shearing yield-stress  $\tau_0 = \sigma_0/2$ , i.e. until  $\tau_{\max} \geq \sigma_0/2$ . Then, from (4.10), the following condition of flow emerges:

$$(\sigma_a - \sigma_r) \geq \sigma_0, \quad (\sigma_0 = \text{yield point of the metal plug}). \quad (4.11)$$

Now, plastic flow occurs in the plug, and the relationship between radial and axial stress in the plug is:

$$\sigma_r = \sigma_a - \sigma_0, \text{ plastic loading} \quad (4.12)$$

At axial pressure release,  $\tau_{\max}$  immediately falls below the level of the shearing yield-stress ( $\tau_{\max} < \sigma_0/2$ ), and the stresses in the metal plug are being released according to:

$$\sigma_r = \sigma_a \nu / (1 - \nu) + k, \text{ elastic releasing } (k = \text{constant}) \quad (4.13)$$

In the course of continued release, the axial stress in the plug decreases and eventually becomes even smaller than the radial stress. From this point on, the following condition of flow rules:

$$(\sigma_r - \sigma_a) \geq \sigma_0 \quad (4.14)$$

and the relationship between radial and axial stress is:

$$\sigma_r = \sigma_a + \sigma_0, \text{ plastic releasing} \quad (4.15)$$

From the above description, it is evident that the entire loading-releasing cycle, which the metal plug undergoes in the compacting die, forms a hysteresis as illustrated in the diagram at *Fig. 4.8 a*.

A particularly interesting detail of this hysteresis is the fact that, after complete release of the axial stress, the plug remains under a compressive radial stress  $\sigma_r$  which is equal to the metals yield point  $\sigma_0$ . In this respect, Long's model provides a plausible

explanation of the spring-back effect ( see § 4.4) occurring when powder compacts are ejected from the compacting die.

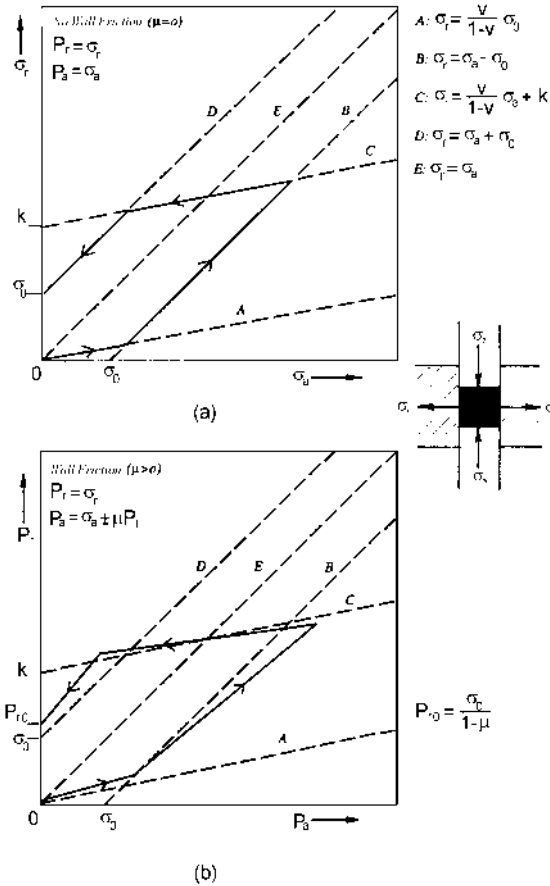


Figure. 4.8.a. Relationship between radial and axial pressure occurring in a cylindrical metal plug inside a rigid die during a cycle of loading and releasing the axial pressure.

(a) Theoretical model disregarding die-wall friction. [4.6 a]

(b) Theoretical model including the aspect of die-wall friction. [4.6 b]

Although Long's model oversimplifies reality in several respects (absence of wall friction, and deformation strengthening), it provides, along general lines, a fairly satisfactory description of the actual relationship between radial and axial pressure occurring when metal powder is being compacted in a rigid die.

Experimental proof of the hysteresis curve predicted by Long's model has been given for several materials by Long himself as well as by other authors. A modified model, suggested by G. Bockstiegel<sup>2</sup>, includes the aspect of die-wall friction as briefly described

below. The frictional forces, occurring at the die wall during powder compacting, act in a direction opposite to the movement of the compacting punch. Thus, while the punch moves in inward direction, the compressive axial stress in the powder  $\sigma_a$  is smaller than the external punch pressure  $P_a$ , and while the punch moves in outward direction,  $\sigma_a$  is larger than  $P_a$ . It can be assumed that the frictional force at the die wall is approximately proportional to the radial pressure  $P_r$  acting upon the die wall. Hence, the following statement is made:

$$\sigma_a = P_a \pm \mu P_r \quad (4.16)$$

The negative sign refers to the phase of pressure increase, the positive sign to the phase of pressure release.  $\mu$  is the frictional coefficient residing at the die wall. The radial pressure upon the die wall  $P_r$  is identical with the radial stress in the powder, i.e.  $P_r = \sigma_r$ .

Introducing (4.16) into Long's equations (4.9), (4.12), (4.13) and (4.15), these are transformed into corresponding equations pertaining to the modified model:

$$P_r = P_a v / (1 - v - \mu v), \text{ elastic loading} \quad (4.9')$$

$$P_r = (P_a - \sigma_0) / (1 + \mu), \text{ plastic loading} \quad (4.12')$$

$$P_r = P_a v / (1 - v + \mu v) + k', \text{ elastic releasing, } (k' = \text{constant}) \quad (4.13')$$

$$P_r = (P_a + \sigma_0) / (1 - \mu), \text{ plastic releasing} \quad (4.15')$$

For  $\mu = 0$  (no wall friction), the modified equations ( ' ) are identical with Long's original equations ( ). Although the modified model is based on a statement which rather simplifies the real conditions of stress and friction at the die wall, it makes evident that the inclusion of wall friction does not change Long's model in its general outlines. The hysteresis curve of the loading-releasing cycle is merely being somewhat distorted. See diagram at *Fig. 4.8 b*.

During the densification of metal powders, the powder mass does not suddenly switch from elastic to plastic behavior as suggested by Long's model, but the transition occurs gradually in the individual powder particles. Apart from this difference, deformation strengthening occurs in the powder particles during densification.

Corresponding to these circumstances, the slope of experimental hysteresis curves changes gradually with increasing pressure instead of suddenly. See example shown at *Fig. 4.9*.

---

<sup>2</sup> G. Bockstiegel, Höganäs 1967



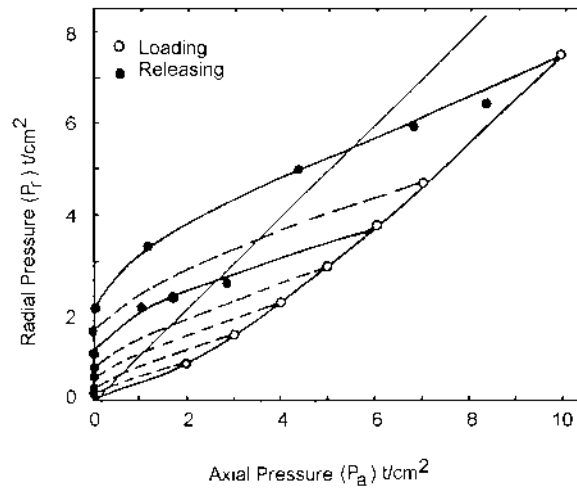


Figure. 4.9. Radial and axial pressures measured on compacts of sponge iron powder during a loading releasing cycle in a cylindrical die. [4.7]

#### 4.2.2 Influence of the Yield Point.

From Long's model, it is evident that the radial pressure, which a metal plug or a mass of metal powder under axial pressure exerts upon the wall of a compacting die, is the smaller the higher the yield point of the metal is. Vice versa, from the same model, it can be concluded that a metal powder with extremely low yield point and negligible tendency to deformation strengthening, like lead powder for instance, should exhibit a nearly hydraulic behavior when compacted in a rigid die.

Experimental proof is in the diagram shown at *Fig. 4.10*. The entire loading-releasing cycle for lead powder does not show any hysteresis, and its very slight deviation from the ideal hydraulic straight line is due to frictional forces at the die wall.

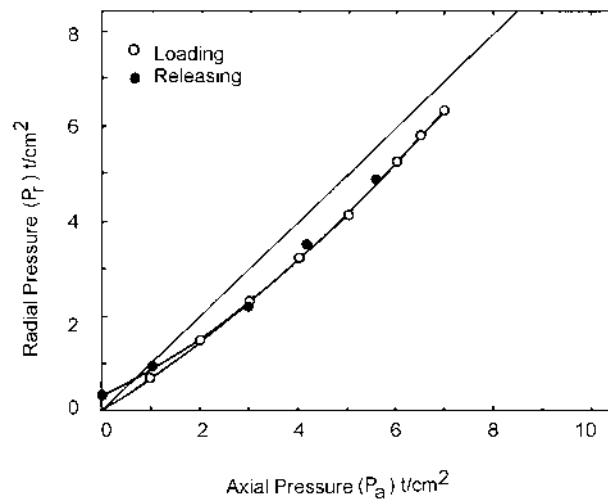


Figure. 4.10. Radial and axial pressures measured on compacts of lead powder during a loading releasing cycle in a cylindrical die. [4.8]

These findings suggest that higher and more homogeneous densities in metal powder compacts could be achieved, if the compacting procedure would be executed at elevated temperatures where the yield point of the metal is lower than at R.T.

Experiments with various iron powder mixes, carried out at the Höganäs laboratory, and pilot production runs, initiated by Höganäs, have proven that already an increase of the powder temperature to 150 - 200°C is sufficient to achieve substantially higher densities and improved properties<sup>3 4</sup>.

The principle influence of a temperature depended yield point on the relationship between axial and radial pressure emerges from the theoretical hysteresis curves shown at *Fig. 4.11*. From these curves, it can be seen that the maximum radial pressure increases but the residual radial pressure, after complete release of the axial pressure, decreases when the yield point is lowered at elevated temperatures.

<sup>3</sup> U. Engström and B. Johansson, Höganäs Iron Powder Information PM 94-9.

<sup>4</sup> J. Tengzelius, Höganäs Iron Powder Information PM 95-2

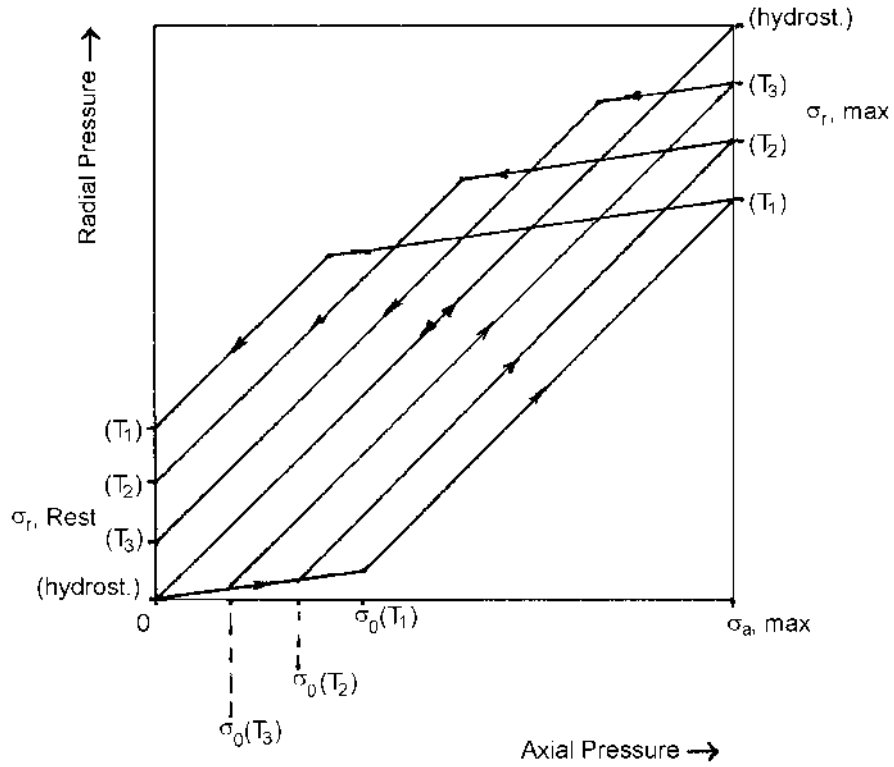


Figure. 4.11. Influence of the yield point  $\sigma_0$  on the relationship between radial and axial pressure for a metal plug inside a cylindrical die during a loading-releasing cycle.

Example: the yield point  $\sigma_0(T)$  decreases with increasing temperature  $T$  ( $T_3 > T_2 > T_1$ ). [4.9]

### 4.3 Axial Density Distribution

Frictional forces at the wall of the compacting die restrain the densification of the powder because they act against the external pressure  $P$  exerted by the compacting punch. With increasing distance from the face of the compacting punch, the axial stress  $\sigma_a$ , available for the local densification of the powder, decreases. This becomes especially adversely apparent in the manufacturing of long thin-walled bushings which at their waist line show substantially lower densities than at their two ends. In order to find an explanation to this phenomenon, we take a closer look at the balance of forces in the powder mass during densification.

We consider densification of powder in a deep cylindrical compacting die with inner diameter  $2r$ . The upper punch is assumed to have entered the die and already compacted the powder to a certain degree so that the axial stress in the powder directly underneath the punch face is  $\sigma_a(0)$ . The variable vertical distance from the punch face be  $x$ . We imagine the powder column in the die as being composed of thin discs stacked upon one another like coins. We select one disc at distance  $x$  from the punch face. Its height be  $dx$ , its cross-sectional area is  $F = \pi r^2$ , and its small lateral area is  $f = 2r\pi dx$ . See sketch at *Fig. 4.12*.

The axial stress, acting upon the top face of this disc, is  $\sigma_a(x)$ . Due to friction between the lateral face of the disc and the die wall, the axial stress  $\sigma_a(x+dx)$ , acting upon the bottom face of the disc, is somewhat smaller than  $\sigma_a(x)$ . We assume that the frictional force is approximately proportional to the axial stress  $\sigma_a(x)$  and to the lateral face  $f$  of the disc. After these preliminaries, we calculate the equilibrium between all forces acting upon the selected disc.

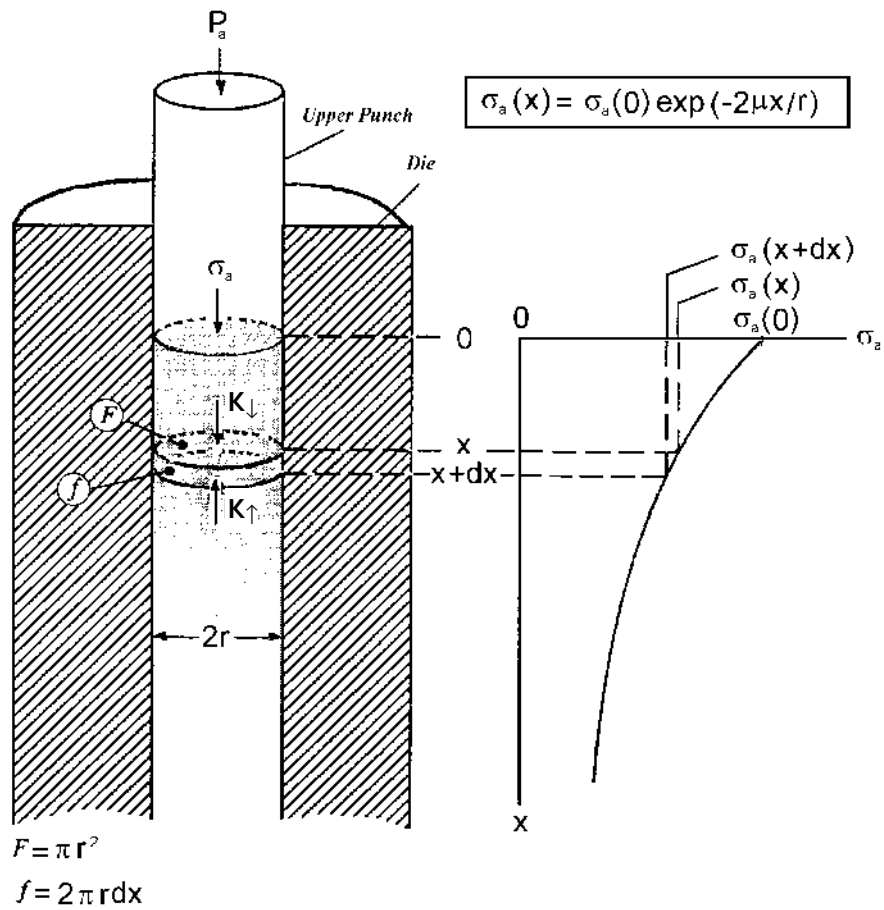


Figure. 4.12. Axial stress  $\sigma_a$  in a powder mass as a function of distance  $x$  from the face of the upper compacting punch. [4.10]

The Force acting upon the top face of the disc is:

$$K_{\downarrow} = \pi r^2 \sigma_a(x) \quad (4.17)$$

The Force acting upon the bottom face of the disc is:

$$K_{\uparrow} = \pi r^2 \sigma_a(x+dx) \quad (4.18)$$

The frictional force acting upon the lateral face of the disc is:

$$K_{\mu} = \mu \pi r^2 dx \sigma_a(x), (\mu = \text{coefficient of friction}) \quad (4.19)$$

Equilibrium of forces resides when

$$K_{\downarrow} - K_{\uparrow} = K_{\mu} \quad (4.20)$$

From (4.17) to (4.20), it follows:

$$d\sigma_a = \sigma_a(x+dx) - \sigma_a(x) = -2\mu \sigma_a(x) dx/r \quad (4.21)$$

Integration of this differential equation yields:

$$\sigma_a(x) = \sigma_a(0) \exp(-2\mu x/r) \quad (4.22)$$

From this equation, it emerges that the axial compressive stress in the powder mass  $\sigma_a(x)$  decreases exponentially with increasing distance  $x$  from the face of moving upper punch, and the more so, the larger the frictional coefficient  $\mu$  and the smaller the inner diameter  $2r$  of the die. The sketch at *Fig. 4.12* illustrates the situation. An exactly equivalent situation arises, of course, in relation to a moving under punch. Thus when a powder is being compacted between symmetrically moving punches (which is usually the case), the axial stresses at both ends of the compact are larger than anywhere mid between.

Consequently, powder compacts usually have a zone of lower density approximately mid between their end faces. This zone of lower density is often referred to as *neutral zone* (ref. to chapter 5). Thus, compacts having thin sections, long in compacting direction, are very fragile before they are sintered.

## 4.4 Ejecting Force and Spring-Back

One direct consequence of the residual radial stress  $\sigma_{r0}$  as discussed in § 4.2.1, is the fact that a substantial force is required to eject a powder compact from the compacting die. Consider a compact of height  $h$  sitting in a cylindrical die having an inner diameter  $2r$ .

Its cross-sectional area is  $F = \pi r^2$ , and its lateral area is  $f = 2\pi r h$ . The frictional coefficient at the die wall be  $\mu$ . Then, the required ejection force is:

$$K_{\uparrow} = \mu \ 2\pi r \ h \ \sigma_{r0} \quad (4.23)$$

and the pressure exerted by the ejecting under punch upon the bottom of the compact is:

$$P_{\uparrow} = K_{\uparrow}/\pi r^2 = \sigma_{r0} \ 4\mu \ h/2r \quad (4.24)$$

According to equation (4.24), the pressure  $P_{\uparrow}$  acting upon the bottom face of the compact during ejection is the higher, the longer the compact is relative to its diameter ( $h/2r$ ). The ejecting pressure is also directly proportional to the frictional coefficient  $\mu$ .

At the onset of the ejecting process, the frictional coefficient  $\mu$  and, consequently, the ejecting pressure  $P_{\uparrow}$  adopt a peak value (adhesive friction) substantially above the "normal" level (sliding friction). See schematic diagram at *Fig. 4.13*. This peak pressure can, in certain cases e.g. with long thin-walled bushings, exceed the maximum pressure that occurred in the compacting process.

This has two consequences:

- (a) A certain re-densification effect occurs at the lower end of the compact.
- (b) A long and slender bottom punch, just strong enough to withstand the compacting load, may yield or break under the ejecting load.

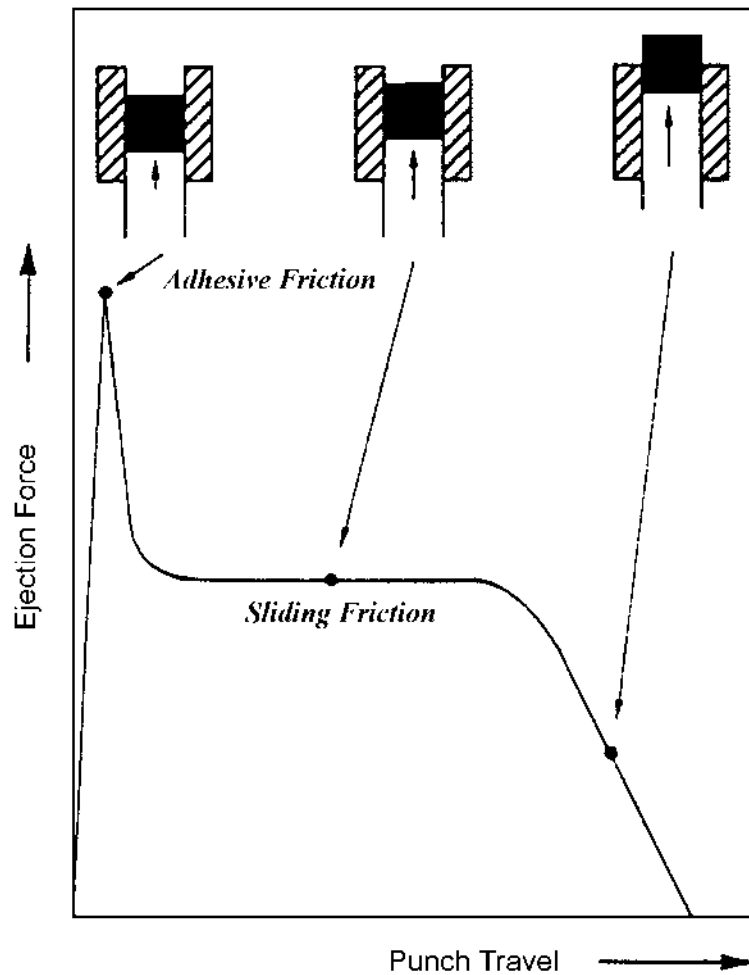


Figure. 4.13. Ejecting force as a function of the movement of the ejecting bottom punch; schematic.

If the wall of the compacting die is worn or insufficiently lubricated, it may come to cold-welding effects between the compact and the die wall, recognizable from an excessive increase of the ejecting pressure and a typical stick-slip behavior (creaking noise). See records from ejecting experiments shown at *Fig. 4.14*.



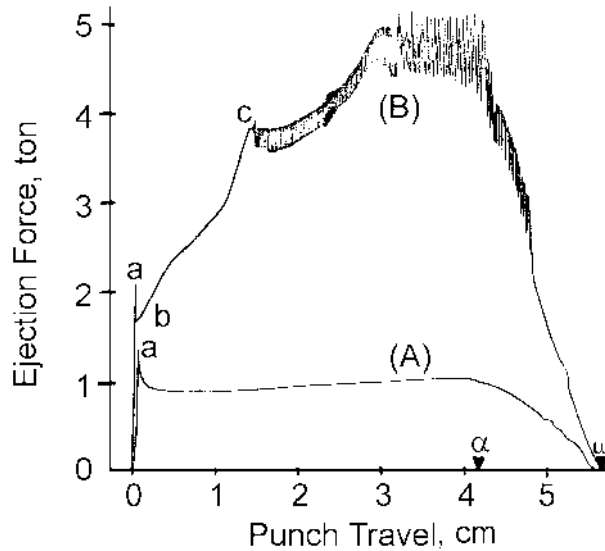


Figure. 414. Influence of the type of lubricant on variations of the ejecting force during ejection of iron powder compacts from a cylindrical hard-metal die having an inner diameter of 25 mm. Powder grade: atomized iron (RZ-type) < 150  $\mu$ m, compacting pressure:  $P_a = 8$  t/cm<sup>2</sup>, compact density:  $d = 7.2$  g/cm<sup>3</sup>, height of compact:  $h = 15$  mm, ejecting speed: 3 mm/s. (A) lubricant: 0.75% Metallub, (B) lubricant: 0.75% Zn-stearate, worn die. (a) adhesive friction peak, (b) begin of sliding friction, (c) severe cold-welding effects between compact and die wall. ( $\alpha$ ) compact begins to leave the die, ( $\omega$ ) compact has left the die. [4.11]

Another consequence of the residual radial pressure becomes apparent at the moment when the compact, on ejection, passes the upper rim of the die. The upper part of the compact, sticking out of the die, expands elastically while the lower part is still under the influence of the residual radial pressure. The horizontal shearing stress arising in this situation may generate horizontal cracks in the compact. In order to diminish the shearing stress and avoid cracks in the compact, it is recommendable to slightly taper the exit of the die and to round the edges of the exit.

The elastic expansion of the compact after ejection from the compacting die is called spring-back and is measured according to the following formula:

$$S(\%) = 100 (\lambda_c - \lambda_d) / \lambda_d \quad (4.25)$$

where  $S(\%)$  = Spring-Back (%),  $\lambda_c$  = transversal dimension of the (ejected) compact,  $\lambda_d$  = corresponding dimension of the compacting die (after ejection of the compact).

The spring-back depends of the following parameters:

- compacting pressure, compacting density
- powder properties
- lubricants and alloying additions
- shape and elastic properties of the compacting die.

The dependence of spring-back on compacting density emerges from the diagram at *Fig. 4.15*. Two important points can be taken from this diagram:

- The powder grade has a strong influence on spring-back. (This must be kept in mind when, in the production of precision structural parts , for one or the other reason, the powder grade is changed).
- At high densities, a small scatter in density entails a wider scatter in spring-back. (This can turn out to have adverse effects on the final tolerances of the sintered structural parts).

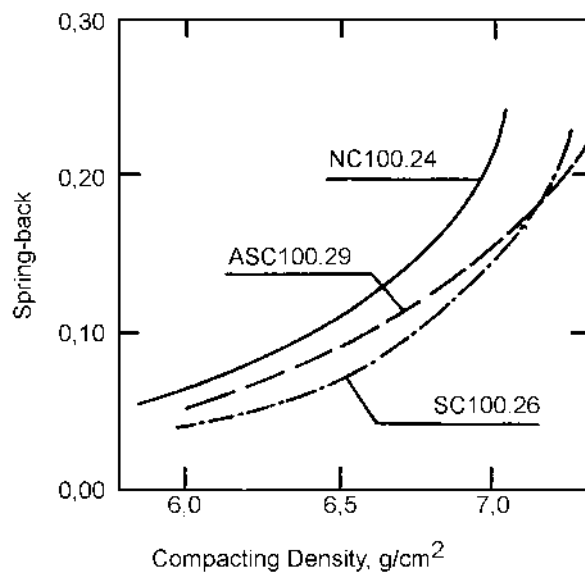


Figure. 4.15: Spring-back as a function of compact density for three different iron powders. Lubricant addition: 0.8% Zn-stearate. [4.12]

## References

- [4.1] Höganäs Data Sheets.
- [4.2] G. Bockstiegel, The Porosity-Pressure Curve and its Relation to the Size Distribution of Pores in Iron Powder Compacts, Proceedings of the 1965 International Powder Metallurgy Conference, New York, NY, USA.
- [4.3] G. Bockstiegel, The Porosity-Pressure Curve and its Relation to the Size Distribution of Pores in Iron Powder Compacts, Proceedings of the 1965 International Powder Metallurgy Conference, New York, NY, USA.
- [4.4] W. Schatt, Pulvermetallurgie, Sinter - und Verbundwerkstoffe, Dr. Alfred Hüthig Verlag, Heidelberg 1988.
- [4.5] G. Bockstiegel, Einfluß des Vor- und Nachpressdruckes sowie der Sintertemperatur auf die Eigenschaften von Sinterteilen aus Eisenpulvern, Archiv für das Eisenhüttenwesen 28 (1957) 3, S.167 -177.
- [4.6 a] W. M. Long, Powder Metallurgy, No. 6, 1960.
- [4.6 b] G. Bockstiegel, Höganäs 1967.
- [4.7] G. Bockstiegel und J. Hewing, Verformungsarbeit, Verfestigung und Seitendruck beim Pressen von Metallpulvern, 2. Europäisches Symposium über Pulvermetallurgie, Stuttgart 1968.
- [4.8] G. Bockstiegel und J. Hewing, Verformungsarbeit, Verfestigung und Seitendruck beim Pressen von Metallpulvern, 2. Europäisches Symposium über Pulvermetallurgie, Stuttgart 1968.
- [4.9] G. Bockstiegel, Höganäs 1967). Example: the yield point  $\sigma_0(T)$  decreases with increasing temperature  $T$  ( $T_3 > T_2 > T_1$ ).
- [4.10] G. Bockstiegel, Höganäs 1967.
- [4.11] G. Bockstiegel, Höganäs 1964.
- [4.12] Höganäs Data Sheets.